



**HAL**  
open science

# Novel Preparation of Cu and Fe Zirconia Supported Catalysts for Selective Catalytic Reduction of NO with NH<sub>3</sub>

Katarzyna Świrk, Ye Wang, Changwei Hu, Li Li, Patrick da Costa, Gerard Delahay

► **To cite this version:**

Katarzyna Świrk, Ye Wang, Changwei Hu, Li Li, Patrick da Costa, et al.. Novel Preparation of Cu and Fe Zirconia Supported Catalysts for Selective Catalytic Reduction of NO with NH<sub>3</sub>. *Catalysts*, 2021, 11 (1), pp.55. 10.3390/catal11010055 . hal-03108567

**HAL Id: hal-03108567**

**<https://hal.science/hal-03108567>**

Submitted on 13 Jan 2021

**HAL** is a multi-disciplinary open access archive for the deposit and dissemination of scientific research documents, whether they are published or not. The documents may come from teaching and research institutions in France or abroad, or from public or private research centers.

L'archive ouverte pluridisciplinaire **HAL**, est destinée au dépôt et à la diffusion de documents scientifiques de niveau recherche, publiés ou non, émanant des établissements d'enseignement et de recherche français ou étrangers, des laboratoires publics ou privés.

Article

# Novel Preparation of Cu and Fe Zirconia Supported Catalysts for Selective Catalytic Reduction of NO with NH<sub>3</sub>

Katarzyna Świrk<sup>1,\*</sup>, Ye Wang<sup>2,3,†</sup>, Changwei Hu<sup>2,4,\*</sup>, Li Li<sup>4</sup>, Patrick Da Costa<sup>3,\*</sup> and Gérard Delahay<sup>1</sup>

<sup>1</sup> Institut Charles Gerhardt Montpellier, Université de Montpellier, ENSCM (MACS), CNRS, 34296 Montpellier, France; gerard.delahay@enscm.fr

<sup>2</sup> College of Chemical Engineering, Sichuan University, Chengdu 610065, China; xihazhezhe@gmail.com

<sup>3</sup> Institut Jean Le Rond d'Alembert, Sorbonne Université, CNRS, 78210 Saint Cyr l'Ecole, France

<sup>4</sup> Key Laboratory of Green Chemistry and Technology, Ministry of Education, College of Chemistry, Sichuan University, Chengdu 610064, China; lili2209362583@163.com

\* Correspondence: katarzyna.swirk@umontpellier.fr (K.Ś.); changwei.hu@scu.edu.cn (C.H.); patrick.da\_costa@sorbonne-universite.fr (P.D.C.); Tel.: +86-28-8541-1105 (C.H.); +33-1-442-79562 (P.D.C.)

† K.Ś. and Y.W. contributed equally.

**Abstract:** Copper and iron promoted ZrO<sub>2</sub> catalysts were prepared by one-pot synthesis using urea. The studied catalysts were characterized by XRD, N<sub>2</sub> physisorption, XPS, NH<sub>3</sub>-TPD, and tested in the selective catalytic reduction of NO with NH<sub>3</sub> (NH<sub>3</sub>-SCR) in the absence and presence of water vapor under the experimental conditions representative of exhaust gases from stationary sources. The influence of SO<sub>2</sub> on catalytic performance was also investigated. Among the studied catalysts, the Fe-Zr sample showed the most promising results in NH<sub>3</sub>-SCR, being active and highly selective to N<sub>2</sub>. The addition of SO<sub>2</sub> markedly improved NO and NH<sub>3</sub> conversions during NH<sub>3</sub>-SCR in the presence of H<sub>2</sub>O. The improvement in acidic surface properties is believed to be the cause.

**Keywords:** zirconia; copper; iron; one-pot synthesis; NH<sub>3</sub>-SCR; NO<sub>x</sub>; acidity



**Citation:** Świrk, K.; Wang, Y.; Hu, C.; Li, L.; Da Costa, P.; Delahay, G. Novel Preparation of Cu and Fe Zirconia Supported Catalysts for Selective Catalytic Reduction of NO with NH<sub>3</sub>. *Catalysts* **2021**, *11*, 55. <https://doi.org/10.3390/catal11010055>

Received: 26 November 2020

Accepted: 30 December 2020

Published: 2 January 2021

**Publisher's Note:** MDPI stays neutral with regard to jurisdictional claims in published maps and institutional affiliations.



**Copyright:** © 2021 by the authors. Licensee MDPI, Basel, Switzerland. This article is an open access article distributed under the terms and conditions of the Creative Commons Attribution (CC BY) license (<https://creativecommons.org/licenses/by/4.0/>).

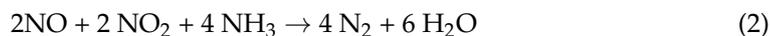
## 1. Introduction

Nitrogen oxides (NO<sub>x</sub>: NO, NO<sub>2</sub>) are known to be major pollutants of the atmosphere. Their emission mainly arises from stationary (fossil fuels combustion) and mobile sources (vehicles), contributing to the formation of photochemical smog, acid rains, and ozone depletion. Different technologies have been used to reduce NO<sub>x</sub> emission [1]. Among them, direct decomposition of NO<sub>x</sub> into N<sub>2</sub> and O<sub>2</sub> is ideal as it only requires a simple contact with the surface of a catalyst. However, the formed oxygen atoms may be strongly adsorbed and cause a rapid deactivation of the catalytic material [2,3]. The second type of technology used for mobile sources is NO<sub>x</sub> Storage/Reduction (NSR) or NO<sub>x</sub> trap [4]. These approaches, however, are limited due to the hydrocarbon and CO<sub>2</sub> penalties caused by cyclic lean-fuel/rich-fuel conditions [5].

The last known technology for NO<sub>x</sub> emission control is the selective catalytic reduction (SCR), including HCs, CO, and H<sub>2</sub>-SCR for automotive pollution processes [6,7]. One of the well-established post-combustion technologies of NO<sub>x</sub> reduction is the selective catalytic reduction of NO<sub>x</sub> with ammonia (NH<sub>3</sub>-SCR). The process has been introduced in the late 1970s, being widely commercialized technology for NO<sub>x</sub> removal from flue gases from coal-fired power plants and other industrial facilities [8,9]. The standard reaction equation for NH<sub>3</sub>-SCR, involving only NO, is given by:



With an equimolar amount of NO and NO<sub>2</sub>, the reaction called fast SCR reaction is much faster, and the reaction equation becomes:



On the other hand, with pure NO<sub>2</sub> the NH<sub>3</sub>-SCR reaction is the slowest and can be presented by the following equation:



The conventional catalysts are V<sub>2</sub>O<sub>5</sub>-WO<sub>3</sub>(MoO<sub>3</sub>)/TiO<sub>2</sub> and Cu, Fe-zeolites [10,11]. In the former, V<sub>2</sub>O<sub>5</sub> represents active phase, whereas WO<sub>3</sub> and MoO<sub>3</sub> increase the temperature window of the SCR reaction and improve the mechanical strength of the catalysts [12]. However, the main drawback of V<sub>2</sub>O<sub>5</sub>-WO<sub>3</sub>(MoO<sub>3</sub>)/TiO<sub>2</sub> is a narrow operating temperature window (300–400 °C), sublimation of vanadium species at high temperatures, and high oxidation of SO<sub>2</sub> to SO<sub>3</sub> leading to a decrease of NO<sub>x</sub> conversion at 400 °C [10]. On the other hand, Cu and Fe zeolites show high activity in a low-temperature window and good hydrothermal resistance [11,13,14]. Both copper ions (Cu<sup>2+</sup> and/or Cu<sup>+</sup>) and iron ions (Fe<sup>3+</sup>) play an important role of active sites in the reaction of NH<sub>3</sub>-SCR. Nevertheless, the application of Cu or Fe zeolites is still challenging as in most cases they are prone to be extensively poisoned by SO<sub>2</sub> [15].

Over the past years, various novel catalysts for NO<sub>x</sub> reduction were described in the literature. Among them, zirconia-supported catalysts were found attractive due to the high thermal stability, high low-temperature activity and durability, as well as enhanced resistance to SO<sub>2</sub> and H<sub>2</sub>O [16–21]. Cu/ZrO<sub>2</sub> and Cu/ZrO<sub>2</sub>(SO<sub>4</sub><sup>2-</sup>) were found very promising in selective catalytic reduction by n-decane [22–24] or propene [25], and finally in NH<sub>3</sub>-SCR [26,27]. Pietrogiacomini et al. [26] prepared the zirconia support by hydrolysis of zirconium oxychloride with ammonia. The obtained carriers were impregnated with aqueous solutions of CuSO<sub>4</sub> or Cu(NO<sub>3</sub>)<sub>2</sub>. Some portion of the latter was additionally sulphurized via gas phase (2770 ppm SO<sub>2</sub> and 1%O<sub>2</sub>, in He). The authors found that impregnation with CuSO<sub>4</sub> or sulphation via gas-phase yielded nearly identical catalysts. CuSO<sub>4</sub>/ZrO<sub>2</sub> were much more selective than the relevant unsulphated CuOx/ZrO<sub>2</sub> to NH<sub>3</sub>-SCR. However, sulphated ZrO<sub>2</sub> catalysts were only slightly more active than unsulphated ZrO<sub>2</sub>.

Iron modified ZrO<sub>2</sub> has been also studied extensively in other catalytic processes [25,28]. According to Apostolescu et al. [18], tetragonal zirconia was the most effective support for Fe catalyst used in NH<sub>3</sub>-SCR when compared to the metal deposited on MgAl<sub>2</sub>O<sub>4</sub>, SiO<sub>2</sub>, or TiO<sub>2</sub>. For Fe/ZrO<sub>2</sub> prepared by sol-gel technique, Navío et al. [29] demonstrated that Fe loading equal or higher than 3 wt% allows to stabilize the zirconia tetragonal phase due to the high solubility of Fe<sup>3+</sup> in the ZrO<sub>2</sub> matrix. By studying NH<sub>3</sub>-SCR of NO over Mn-Fe supported catalysts, López-Hernández et al. [30] showed that acidity is necessary to catalyze the reaction, but not sufficient to obtain the most effective material. The authors showed a significant relationship between SCR activity at low temperatures and surface area through the better iron dispersion for the supports with Lewis acid properties (zirconia, alumina and titania). Since iron oxide also possesses Lewis acidity, resulting catalysts are in principle less sensitive to deactivation of the Brønsted acid sites. Considering this point, Kustov et al. [31] studied the effect of potassium on vanadium, copper, and iron oxides supported on sulphated zirconia (monoclinic), where a slight increase in alkali resistance was found compared to the vanadium.

Indovina et al. [32] examined FeOx/sulphated-ZrO<sub>2</sub> and FeOx/ZrO<sub>2</sub> prepared by impregnation of different Fe precursors. The authors have found that iron species were much less reducible in FeOx/sulphated-ZrO<sub>2</sub> than in FeOx/ZrO<sub>2</sub>. Their lower reducibility explained why FeOx/sulphated-ZrO<sub>2</sub> samples may achieve higher selectivity for the selective catalytic reduction of NO with NH<sub>3</sub>.

Fan et al. [33] investigated sulphated iron-based catalysts prepared by impregnation methods through changing the loading order of  $\text{Fe}_2\text{O}_3$  and  $\text{SO}_4^{2-}$  on  $\text{ZrO}_2$  carrier. The activities of sulphate Fe-based catalysts improved significantly compared to the Fe/Zr catalyst, when tested in the temperature range of 250–500 °C. The authors showed that sulphate supplied higher number of acid sites, which could adsorb more  $\text{NH}_3$  species that can react with gaseous  $\text{NO} + \text{O}_2$ . Recently, Liu et al. [34] investigated the selective catalytic reduction of  $\text{NO}_x$  with ammonia over sulphated iron-based catalysts in using different loadings of  $\text{Fe}^{3+}$  and  $\text{SO}_4^{2-}$  on zirconia support. Their results indicated that the interaction between  $\text{Fe}^{3+}$  and  $\text{SO}_4^{2-}$  can have an effect on the redox ability, acid sites, and adsorption of  $\text{NO}_x$  and  $\text{NH}_3$ . By increasing the content of  $\text{Fe}^{3+}$ , the redox activity of the catalyst and the adsorption of ammonia improved at medium and low temperatures, whereas at higher temperatures, the increase in  $\text{Fe}^{3+}$  species led to the decrease in the conversion of  $\text{NO}_x$  due to the enhancement of the  $\text{NH}_3$  oxidation.

In this work, a novel one-pot synthesis was proposed for the preparation of zirconia-supported Cu and Fe catalysts. The catalysts were tested in selective catalytic reduction of  $\text{NO}$  with  $\text{NH}_3$  in the presence and absence of water vapor. Physicochemical properties of catalysts were examined by  $\text{N}_2$  physisorption, X-ray diffraction (XRD), X-ray photoelectron spectroscopy (XPS), and temperature-programmed desorption of  $\text{NH}_3$  ( $\text{NH}_3$ -TPD). The characterized materials were tested in  $\text{NH}_3$ -SCR (with or without  $\text{H}_2\text{O}$ ). The activity changes during  $\text{SO}_2$  feeding (in situ sulphation) were studied at 450 °C. Additionally, the activity towards  $\text{NH}_3$ -SCO (with or without  $\text{H}_2\text{O}$ ) was also investigated. The importance of support morphology and phase was highlighted.

## 2. Results and Discussion

### 2.1. Catalysts Characterization

#### 2.1.1. Structural and Textural Properties of $\text{ZrO}_2$ Supported Catalysts

The structure of the studied samples was determined by XRD, as presented in Figure 1 and Table 1. The reflections at  $2\theta$  ca. 30.1, 35.2, 60.4, 62.9, 74.8, 81.9, and 85.6° were attributed to the tetragonal  $\text{ZrO}_2$  (t- $\text{ZrO}_2$  indication) [35–38]. In all studied catalysts, only  $\text{ZrO}_2$  diffraction peaks were observed. The absence of diffraction peaks attributed to iron or copper species suggests their good dispersion or insertion into the skeleton of  $\text{ZrO}_2$  [39,40]. The latter can be supported by a small shift to higher Bragg angles observed for Cu-Zr (30.376°) and Fe-Zr (30.349°) catalysts, compared to the  $\text{ZrO}_2$  support (30.192°). Moreover, the d-spacing decreased from 2.9576 Å ( $\text{ZrO}_2$ ) to 2.9402 Å (Cu-Zr) or 2.9427 Å (Fe-Zr). Generally, the ionic radii are influenced by coordination number and valence. Shannon [41] found a correlation between the coordination number and the ionic radius. The ionic radius of  $\text{Zr}^{4+}$  in  $\text{ZrO}_2$  (0.86 Å) is higher than that of  $\text{Fe}^{3+}$  in  $\text{Fe}_2\text{O}_3$  (0.69 Å) or  $\text{Cu}^{2+}$  in  $\text{CuO}$  (0.60 Å) [42]. Probably some  $\text{Zr}^{4+}$  ions were substituted by  $\text{Cu}^{2+}$  or  $\text{Fe}^{3+}$  to form  $\text{CuO-ZrO}_2$  or  $\text{Fe}_2\text{O}_3\text{-ZrO}_2$  solid solutions in the lattice sites. This could be a consequence of the shrink of the lattice parameter [43], which is in line with the XRD results. The shift towards higher Bragg angles was more pronounced for the Cu-Zr catalyst when compared to the Fe-Zr. The crystallite size of  $\text{ZrO}_2$  was calculated by the Williamson and Hall method [44,45]. One can note that the crystallite size of  $\text{ZrO}_2$  decreased, from 13.7 nm to 11.3 and 8.8 nm for Cu-Zr and Fe-Zr catalysts, respectively.

**Table 1.** Structural and textural properties of  $\text{ZrO}_2$ , Cu-Zr and Fe-Zr calcined catalyst.

Sample	Bragg Angles/°	d-Spacing/Å	Crystallite Size of $\text{ZrO}_2$ /nm *	Specific Surface Area/ $\text{m}^2/\text{g}$	Volume of Mesopores/ $\text{cm}^3/\text{g}$	Average Pore Size/nm
$\text{ZrO}_2$	30.192	2.9576	13.7	81	0.12	5.0
Cu-Zr	30.376	2.9402	11.3	128	0.06	3.3
Fe-Zr	30.349	2.9427	8.8	139	0.09	3.5

\* calculated by the Williamson and Hall method.

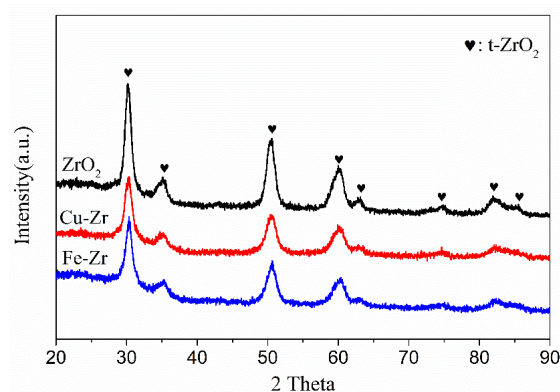


**Figure 1.** X-ray diffraction (XRD) diffractograms of  $\text{ZrO}_2$  support, Cu-Zr and Fe-Zr calcined catalysts.

$\text{N}_2$  physisorption was employed to determine the textural properties of the synthesized catalysts. The analysis was performed for the calcined materials. The samples were found mesoporous with the Barrett–Joyner–Halenda (BJH) mesopore volume ranged from 0.12 to 0.06  $\text{cm}^3/\text{g}$ , average pore size of 3.3–5 nm, and the surface area from 81 to 139  $\text{m}^2/\text{g}$ . These textural parameters decreased and increased with metal modification, meaning that presence of Cu and Fe led to the enhancement of specific surface area with formation of smaller mesopores with less volume.

#### 2.1.2. Acidic Properties of $\text{ZrO}_2$ Supported Catalysts

The total acidity of the studied catalysts was evaluated by  $\text{NH}_3$  temperature programmed desorption ( $\text{NH}_3$ -TPD). Figure 2 presents the desorption curves for the studied catalysts. All samples showed a wide  $\text{NH}_3$  desorption profiles between 100 and 550  $^\circ\text{C}$ , arising from weak (ca. 200  $^\circ\text{C}$ ), medium (ca. 300–400  $^\circ\text{C}$ ), and strong ( $T > 400$   $^\circ\text{C}$ ) acid sites [46,47]. The modification of  $\text{ZrO}_2$  with copper and iron influenced the acidic properties by offering new weak and medium acid sites. Accordingly, the total acidity increased for Cu- and Fe-containing samples in contrast to the unmodified support. These observations are in line with the previously published reports on Cu/ $\text{ZrO}_2$  and Fe/ $\text{ZrO}_2$  materials. Pietrogiacomi et al. [26] reported higher total amount of desorbed ammonia for ZCu2.5 sample than for  $\text{ZrO}_2$  (0.5 vs. 0.2  $\text{nm}^{-1}$ ). Ismail et al. [28] observed the formation of new acidic sites on  $\text{ZrO}_2$  surface due to the Fe addition (1.25, 2.5, 5, and 10 wt%). The authors, however, reported increasing intensities of the desorption profiles in the wide-ranging temperature window (from 200 to 500  $^\circ\text{C}$ ). In the other study of these authors [46], the modification with iron led to the formation of new strong acid sites only ( $T > 400$   $^\circ\text{C}$ ) in comparison to the acid sites recorded for pure zirconia.

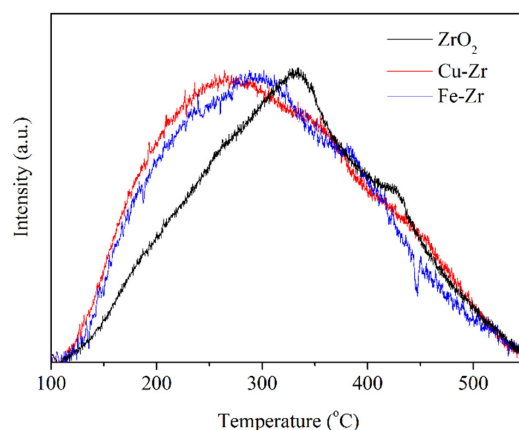


**Figure 2.** Temperature-programmed desorption of  $\text{NH}_3$  ( $\text{NH}_3$ -TPD) profiles of  $\text{ZrO}_2$  support, Cu-Zr and Fe-Zr calcined catalysts.

### 2.1.3. Surface Properties of ZrO<sub>2</sub> Supported Catalysts

The surface composition of the calcined samples was analyzed by XPS. Figure 3A–D present the obtained spectra for O 1s, Zr 3d, Fe 2p, and Cu 2p. The percentage values of the elements are listed in Table 2. ZrO<sub>2</sub> support and Cu-Zr catalyst showed similar content of Zr species on the surface, whereas the percentage of Zr species decreased from 66.8 wt% (ZrO<sub>2</sub> support) to 64.4 wt% for Fe-Zr. The content of surface Cu species is about 2.2 wt%, which is lower than the assumed content (3 wt%). One can assume that part of Cu species could exist in the framework of ZrO<sub>2</sub> or in the bulk. On the contrary, the percentage of Fe species is 3.2 wt%, indicating that more Fe species are formed on the surface than the interior of ZrO<sub>2</sub> catalyst. Thus, the higher content of surface Fe species may contribute to increased activity in NH<sub>3</sub>-SCR of NO into N<sub>2</sub>. Besides, the O 1s curve was resolved into three peaks, which are attributed to lattice oxygen (O<sup>2-</sup>), carbonate species (CO<sub>3</sub><sup>2-</sup>) and hydroxyl species (OH<sup>-</sup>) [43,48]. The Zr 3d was deconvoluted into Zr<sup>3+</sup> and Zr<sup>4+</sup> species as reported elsewhere [49]. The content of each deconvoluted peak is listed in Table 2. The peak of O 1s on Fe-Zr catalyst shifts to lower binding energy in contrast to ZrO<sub>2</sub> support and Cu-Zr catalyst. There are two possible reasons of this observation: (i) higher content of lattice oxygen species on Fe-Zr catalyst, or (ii) less interaction between O<sup>2-</sup> species and Fe due to an exposure of Fe<sub>2</sub>O<sub>3</sub> and/or FeO species on the surface. Similar results were reported in literature [48,50]. Moreover, in our materials the content of Zr<sup>4+</sup> species decreased from 62.5% to 57.2% and 4.7% by introduction of Cu or Fe, respectively, indicating that the presence of Cu or Fe results in higher content of Zr<sup>3+</sup> species on the catalysts. This effect was more pronounced for Fe-Zr catalyst showing 95.3% of Zr<sup>3+</sup> species. It additionally implies that Cu or Fe could promote the formation of Zr species with lower valence value. Furthermore, according to Zhao et al. [48], the curve of Fe 2p and Cu 2p are resolved to Fe<sup>2+</sup> and Fe<sup>3+</sup> species, and Cu<sup>+</sup> and Cu<sup>2+</sup> species, respectively. In our study, the ratio of Fe<sup>2+</sup>/Fe<sup>3+</sup> is 1.33, and the Cu<sup>+</sup>/Cu<sup>2+</sup> is 3.84. This indicates that more Fe species are present in higher valence state on Fe-Zr catalyst, corresponding to higher content of Zr<sup>3+</sup> species. Moreover, recently on functionalized iron hydroxyapatite catalysts it was clearly shown that the presence of Fe<sup>3+</sup> highly dispersed on the surface led to a high selectivity to N<sub>2</sub>, a satisfactory activity in a wide temperature window [41] and improved catalytic activity [34].

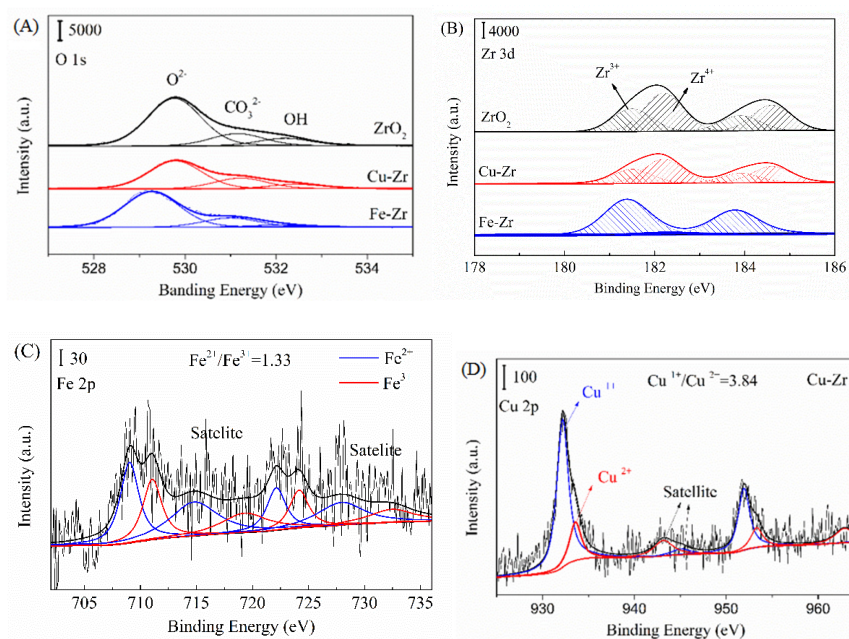


**Figure 3.** X-ray photoelectron spectroscopy (XPS) profiles of ZrO<sub>2</sub> support, Cu-Zr and Fe-Zr calcined catalysts. (A) The O 1s, (B) Zr 3d, (C) Fe 2p, and (D) Cu 2p. All the data are referenced using the C 1s peak at 284.6 eV.

**Table 2.** Elemental composition of ZrO<sub>2</sub>, Cu-Zr calcined catalyst and Fe-Zr calcined catalyst from XPS analysis.

Sample	Zr (wt%)	O (wt%)	Cu (wt%)	Fe (wt%)	O Species (%)			Zr Species (%)	
					O <sup>2-</sup>	CO <sub>3</sub> <sup>2-</sup>	OH <sup>-</sup>	Zr <sup>3+</sup>	Zr <sup>4+</sup>
ZrO <sub>2</sub>	66.8	33.2	-	-	70.6	18.1	11.3	37.5	62.5
Cu-Zr	66.6	31.2	2.2	-	64.9	24.7	10.4	42.8	57.2
Fe-Zr	64.4	32.4	-	3.2	75.8	19.9	4.3	95.3	4.7

## 2.2. Catalytic Results

### 2.2.1. NH<sub>3</sub>-SCR of NO in the Absence and Presence of Water Vapor

Figure 4 shows the catalytic performance of Cu-Zr and Fe-Zr catalysts and the support in NH<sub>3</sub>-SCR of NO as function of temperature. The tests were performed in the presence (3.5 vol%) and in absence of water vapor.

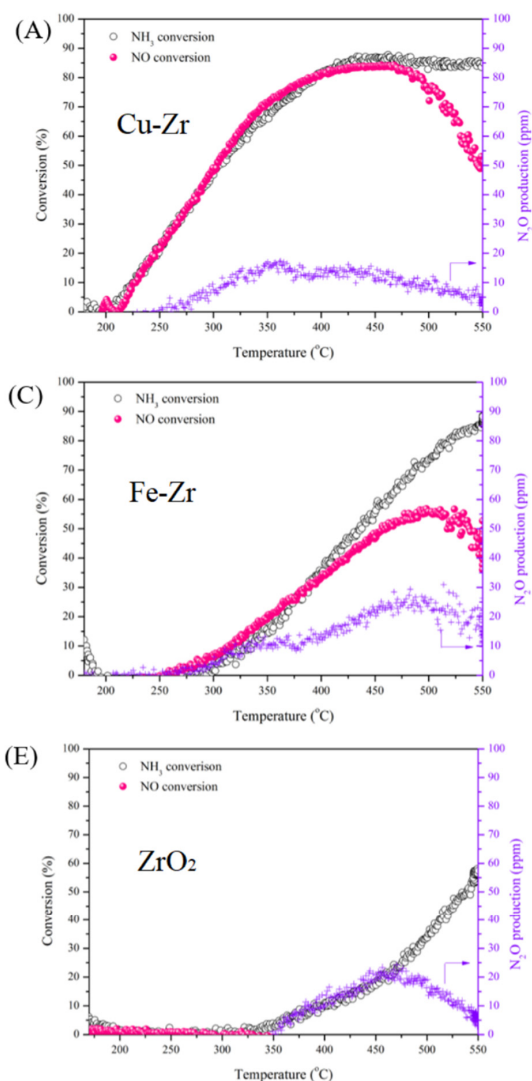
Figure 4A,B presents catalytic results of Cu-Zr catalyst. The catalyst revealed maximum NO conversion of 85% in the absence, and 40% in the presence of H<sub>2</sub>O at 450 °C. In the former conditions, the obtained conversions were two times higher than those observed by Pietrogiacomini et al. [27] (700 ppm NO, 700 ppm NH<sub>3</sub>, 36,000 ppm O<sub>2</sub>, balance He, GHSV = 10<sup>5</sup> h<sup>-1</sup>) on impregnated Cu/ZrO<sub>2</sub> catalysts, which clearly shows that the newly used synthesis would be a good alternative for such type of catalysts. Above 450 °C, the NO conversion rapidly decreased, suggesting an excess production of nitric oxide which could originate from a significant contribution of NH<sub>3</sub> oxidation reaction. This agrees with NH<sub>3</sub> conversion which remained stable, or it increased constantly above 450 °C. The impact of NH<sub>3</sub> oxidation will be studied by us further in this section. The production of N<sub>2</sub>O was minor, showing only max 20 ppm when sample was tested without water vapor, and 10 ppm when test was performed in hydrothermal conditions.

Figure 4C,D shows the NH<sub>3</sub>-SCR over Fe-Zr catalyst. The absence of water vapor led to a maximum of 55% of NO conversion at 500 °C. The N<sub>2</sub>O production was measured at ca. 28 ppm at this temperature. The presence of H<sub>2</sub>O resulted in a constant increase of NO and NH<sub>3</sub> conversions, starting from 300 to 550 °C. At the latter temperature, the NO and NH<sub>3</sub> conversions are 35 and 53%, respectively. The decrease of activity, in the presence of H<sub>2</sub>O, is believed to be mainly due to competing adsorption between water and ammonia on the acid sites [51]. It should be mentioned, additionally, that in the presence of H<sub>2</sub>O, the Fe-Zr catalyst did not produce N<sub>2</sub>O over the whole range of studied temperatures.

From Figure 4E, one can note that the support is inactive during NH<sub>3</sub>-SCR reaction as only conversion of NH<sub>3</sub> was observed accompanied by the production of N<sub>2</sub>O and NO. Negative conversion values were recorded for the latter (not shown in Figure 4E). These observations suggest that selective oxidation of ammonia is a dominant reaction for the support. ZrO<sub>2</sub> support tested in the hydrothermal conditions led to the complete inhibition of any significant catalytic reaction below 500 °C. However, some NH<sub>3</sub> conversion, not exceeding 10% at 550 °C, occurred above 500 °C.

Furthermore, N<sub>2</sub>O is the only by-product detected during the NH<sub>3</sub>-SCR process, which determines selectivity to N<sub>2</sub> presented in Figure 5. As shown in Figure 4B,D, the presence of water leads to a decrease in NO conversion but improves, despite this, the removal efficiency of NO by enhancing the selectivity to N<sub>2</sub>. In the whole SCR process, the N<sub>2</sub>O concentration detected during the tests in presence of water is very limited for Cu-Zr catalyst and negligible for Fe-Zr catalyst. Therefore, one can conclude that Fe-Zr could be a promising catalyst for NH<sub>3</sub>-SCR process after its optimization. This higher catalytic performance could be linked with the increase of electron transfer on Fe-Zr catalysts showed by XPS when compared to the Cu-Zr system. In order to confirm these promising results on Fe-Zr catalysts, selective catalytic oxidation of ammonia (NH<sub>3</sub>-SCO) was performed.

[NO] = [NH<sub>3</sub>] = 1000 ppm, [O<sub>2</sub>] = 2.5 vol%, He as balance



[NO] = [NH<sub>3</sub>] = 1000 ppm, [O<sub>2</sub>] = 2.5 vol%, [H<sub>2</sub>O] = 3.5%, He as balance

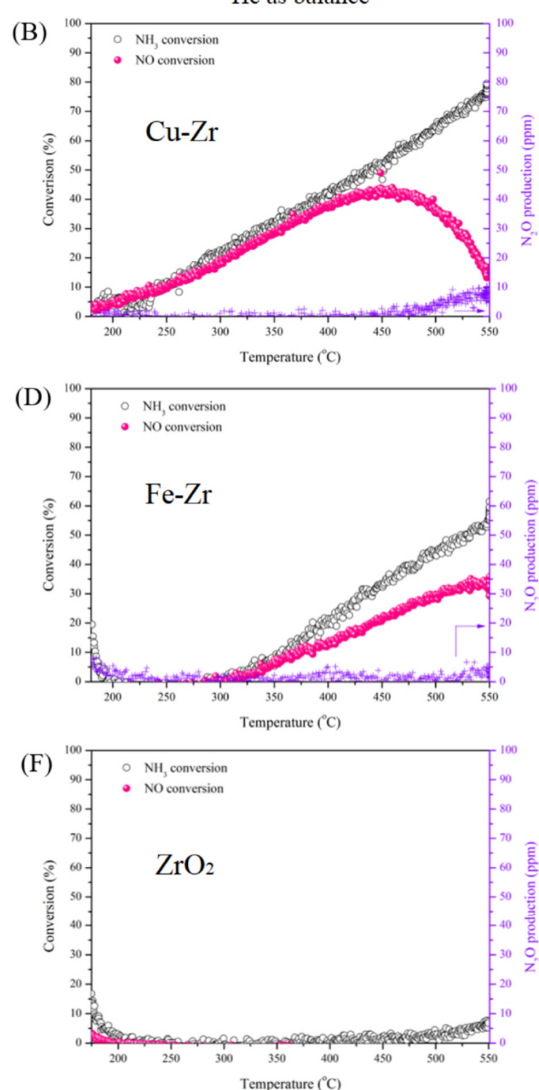


**Figure 4.** NO and NH<sub>3</sub> conversion profiles and N<sub>2</sub>O production as a function of temperature in NH<sub>3</sub>-SCR over Cu-Zr catalyst (A) in absence of water, (B) in presence of water, Fe-Zr catalyst (C) in absence of water, (D) in presence of water, and ZrO<sub>2</sub> support (E) in absence of water, (F) in presence of water. The experimental conditions: [NO] = 1000 ppm, [NH<sub>3</sub>] = 1000 ppm, [H<sub>2</sub>O] = 3.5 vol% when used, [O<sub>2</sub>] = 2.5 vol% diluted in helium; total flowrate of 100 mL/min.

### 2.2.2. NH<sub>3</sub>-SCO in the Absence and Presence of Water Vapor

The selective catalytic NH<sub>3</sub> oxidation (SCO) ability of a catalyst determines the efficiency of NH<sub>3</sub> utilization in the SCR reaction. Figure 5A–F depicts the NH<sub>3</sub> oxidation performance of the studied materials in the absence and presence of H<sub>2</sub>O. Cu-Zr catalyst shows high ammonia oxidation activity starting from 325 °C, reaching constant value of 87% at 450–550 °C (Figure 6A). The oxidation of NH<sub>3</sub> led to N<sub>2</sub>O and NO by-products formation with maximum values of 38 ppm and 250 ppm, respectively. In the hydrothermal conditions, the Cu-Zr catalyst was less active in NH<sub>3</sub>-SCO, compared to the conditions without water vapor (Figure 6B). NH<sub>3</sub> conversion constantly increased over the studied temperatures with a maximum of 68% at 550 °C. Iron promoted ZrO<sub>2</sub> was also active in NH<sub>3</sub>-SCO with 89% of NH<sub>3</sub> at 550 °C complemented by the production of N<sub>2</sub>, N<sub>2</sub>O, and

NO (Supplementary Materials Figure S1; Figure 6C). Ammonia oxidation in the presence of H<sub>2</sub>O led to the decreased activity with only 28% of NH<sub>3</sub> converted (Figure 6D) and low production of side products, i.e., N<sub>2</sub>O and NO. Figure 5E presents zirconia support which was active in NH<sub>3</sub>-SCO, resulting mostly in the production of NO (400 ppm) at the highest analyzed temperature. Small amounts of N<sub>2</sub>O were also observed (10 ppm). The presence of water in ammonia oxidation inhibited reaction, and only 5% of NH<sub>3</sub> conversion was observed (Figure 6F). When compared to NH<sub>3</sub>-SCR results, one can conclude that NH<sub>3</sub> oxidation is predominant at high temperature (T > 400 °C) over Cu-Zr and Fe-Zr catalysts. In contrast, during the hydrothermal conditions the adsorbed NH<sub>3</sub> is more difficult to be oxidized on the surface of both Cu-Zr and Fe-Zr catalysts. Therefore, the adsorbed NH<sub>3</sub> species can effectively react with NO, giving a high NO removal efficiency.

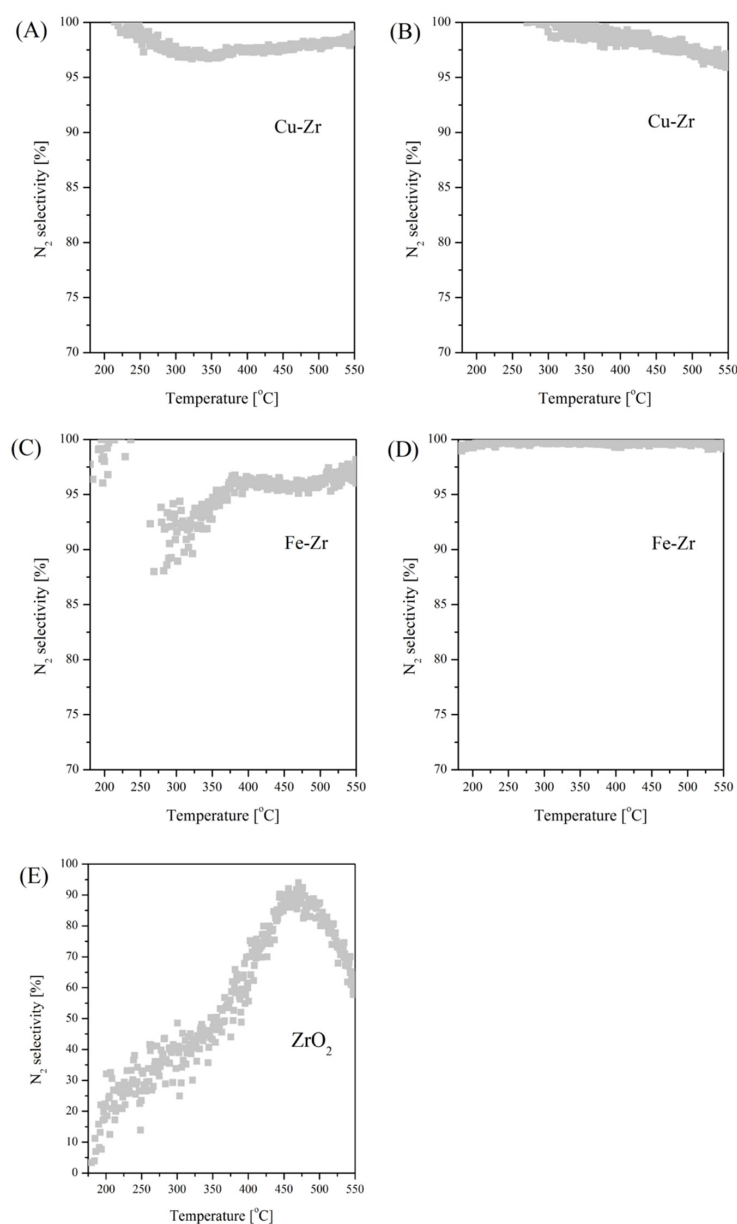


**Figure 5.** N<sub>2</sub> selectivity as a function of temperature measured during NH<sub>3</sub>-SCR over Cu-Zr catalyst (A) in absence of water, (B) in presence of water, Fe-Zr catalyst (C) in absence of water, (D) in presence of water, and ZrO<sub>2</sub> support (E) in absence of water. The experimental conditions: [NO] = 1000 ppm, [NH<sub>3</sub>] = 1000 ppm, [H<sub>2</sub>O] = 3.5 vol% when used, [O<sub>2</sub>] = 2.5 vol% diluted in helium; total flowrate of 100 mL/min.

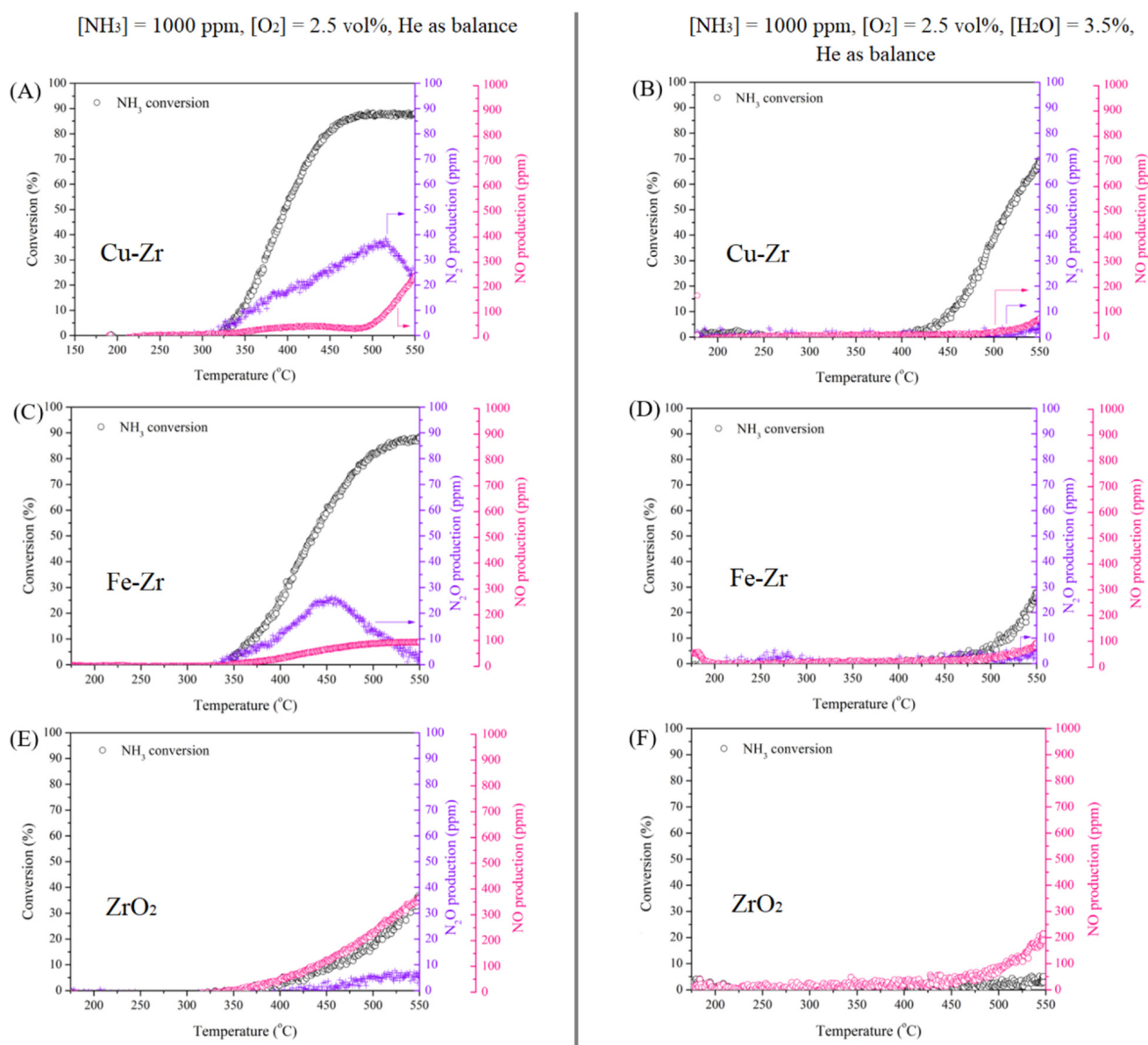


**Figure 6.** NH<sub>3</sub> conversion profile and N<sub>2</sub>O and NO production profiles as a function of temperature in NH<sub>3</sub>-SCO over Cu-Zr catalyst (A) in absence of water, (B) in presence of water; Fe-Zr catalyst (C) in absence of water, (D) in presence of water; and ZrO<sub>2</sub> support (E) in absence of water, (F) in presence of water. The experimental conditions: [NH<sub>3</sub>] = 1000 ppm, [H<sub>2</sub>O] = 3.5 vol% when used, [O<sub>2</sub>] = 2.5 vol% diluted in helium; total flowrate of 100 mL/min.

### 2.2.3. SO<sub>2</sub> Activation of Cu-Zr and Fe-Zr Catalysts and their Catalytic Behavior in NH<sub>3</sub>-SCR of NO in the Absence and Presence of Water Vapor

#### SO<sub>2</sub> Activation of Cu-Zr Catalyst in NH<sub>3</sub>-SCR of NO in the Absence of Water Vapor

The SO<sub>2</sub> activation study in NH<sub>3</sub>-SCR of NO in the absence of H<sub>2</sub>O was carried out on Cu-Zr catalyst at 450 °C. Prior to this examination, the reaction of NH<sub>3</sub>-SCR of NO was performed as a function of temperature, which agrees well with previously obtained results (Figure 4A). Subsequently, the sample was allowed to be stabilized for 60 min before the addition of SO<sub>2</sub> for another 60 min, and then after removing the SO<sub>2</sub> for next 90 min. When the SO<sub>2</sub> was added, a clear increase in both NH<sub>3</sub> and NO conversions was observed resulting in ca. 100% (Figure 7). Once the SO<sub>2</sub> was removed from the feed, a rapid decrease was registered for both, steadying the values to be initially slightly

higher than those registered before  $\text{SO}_2$  feeding. Over the stabilization in the mixture free of  $\text{SO}_2$ , the conversions gradually increased from 83.7 to 90.5% and 83.9 to 85.7% for  $\text{NO}$  and  $\text{NH}_3$  conversions, respectively. The in-situ sulphation promoted the activity of Cu-Zr catalyst in  $\text{NH}_3$ -SCR of  $\text{NO}$ . Similar observations were made in the studies of Pietrogiacomini et al. [26,27] in which it has been reported that sulphation of Cu-containing  $\text{ZrO}_2$  catalysts positively affects catalytic performance  $\text{NH}_3$ -SCR of  $\text{NO}$  due to the enhanced acidic properties of sulphated supports.

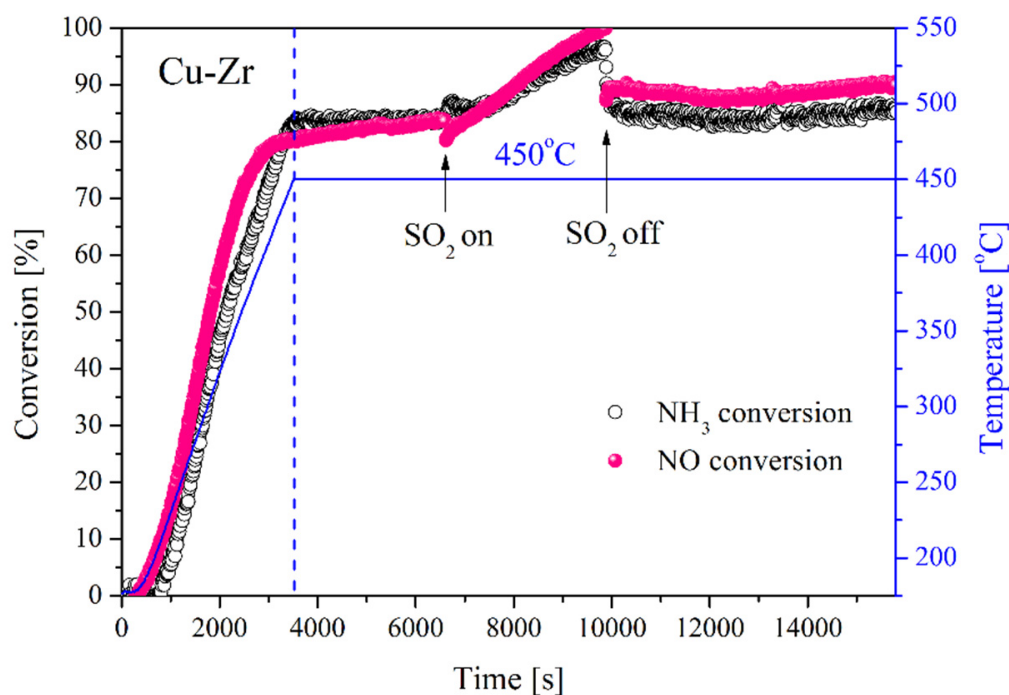


**Figure 7.** Effect of  $\text{SO}_2$  addition during  $\text{NH}_3$ -SCR over Cu-Zr catalyst in the absence of water. The experimental conditions:  $[\text{NO}] = [\text{NH}_3] = 1000$  ppm,  $[\text{SO}_2] = 100$  ppm when used,  $[\text{O}_2] = 2.5$  vol% diluted in helium; total flowrate of 100 mL/min.

#### $\text{SO}_2$ Activation of Fe-Zr in $\text{NH}_3$ -SCR of $\text{NO}$ in the Presence of Water Vapor

Recently, Fan et al. [33] showed that Fe/ $\text{ZrO}_2$  sulphated catalysts were almost two times more active than non-sulphated Fe/ $\text{ZrO}_2$  in  $\text{NH}_3$ -SCR of  $\text{NO}$ . Thus, in order to verify the activation of the catalysts in the presence of  $\text{SO}_2$ , the experiment was performed in hydrothermal conditions over Fe-Zr catalyst and over the support. The results are presented in Figure 8A,B. In the presence of water, an interesting trend was observed for the Fe-Zr catalyst (Figure 8A). During the first hour of stabilization, the conversions of  $\text{NO}$  and  $\text{NH}_3$  were 29% and 30%, respectively. After  $\text{SO}_2$  addition, a slight decrease of  $\text{NO}$  and  $\text{NH}_3$  was observed, probably due to the sulphation of the Fe-Zr and inhibition of the active sites. However, after the first minutes in the presence of  $\text{SO}_2$ , both conversions of  $\text{NO}$  and  $\text{NH}_3$  increased. It is worth to note that the consumption of  $\text{NH}_3$  reached 47%, whereas only 30% of  $\text{NO}$  was converted. This latter result could not be linked with any  $\text{NH}_3$  oxidation activity, despite the high temperature of 450 °C. No side products were recorded by MS that could suggest  $\text{NH}_3$ -SCO occurrence. Moreover, on the  $\text{ZrO}_2$  support a similar  $\text{NH}_3$  consumption was registered (Figure 8B). One can assume that ammonia consumption is mainly due to its adsorption enhanced by a formation of new acidic sites in the presence of  $\text{SO}_2$  which can act as a reservoir [33]. Similar observations were made on other type of catalysts such as  $\text{V}_2\text{O}_5\text{-WO}_3/\text{TiO}_2$  [52–54].

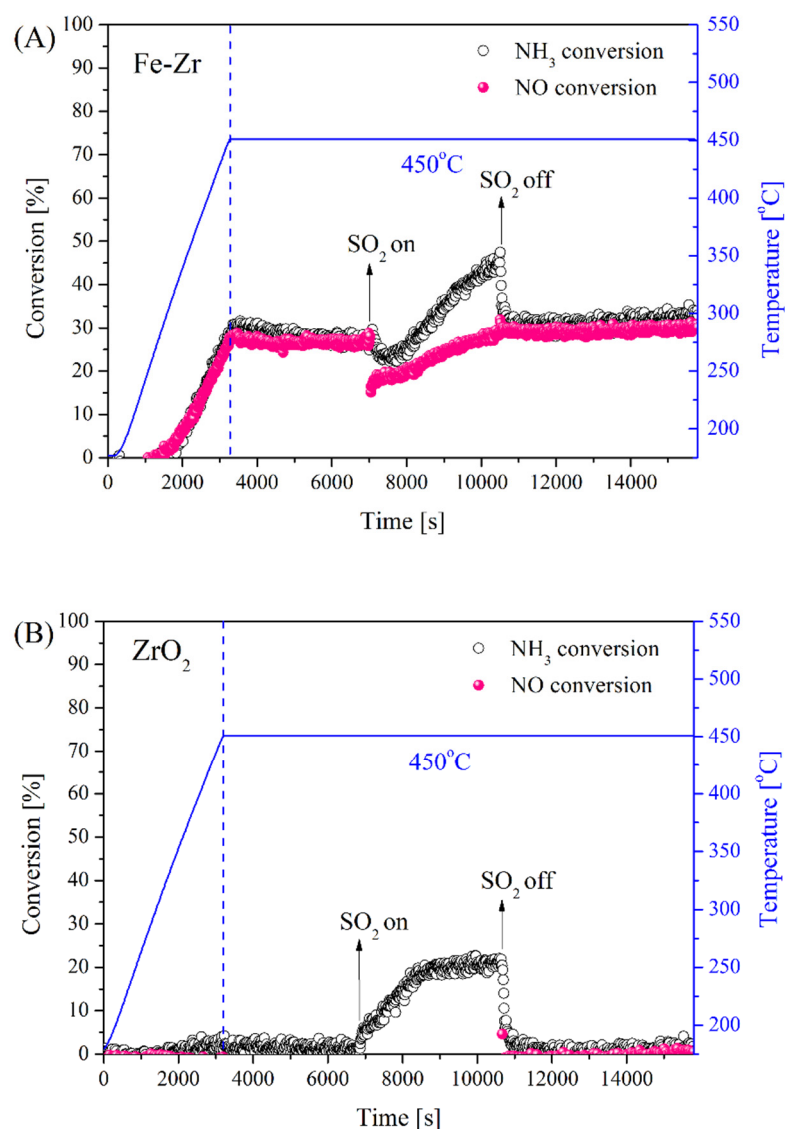


**Figure 8.** Effect of SO<sub>2</sub> addition during NH<sub>3</sub>-SCR over Fe-Zr and ZrO<sub>2</sub> catalysts in the hydrothermal conditions. (A) Fe-Zr catalyst, (B) ZrO<sub>2</sub> support. The experimental conditions: [NO] = [NH<sub>3</sub>] = 1000 ppm, [SO<sub>2</sub>] = 100 ppm when used, [H<sub>2</sub>O] = 3.5 vol%, [O<sub>2</sub>] = 2.5 vol% diluted in helium; total flowrate of 100 mL/min.

### 3. Materials and Methods

#### 3.1. Catalysts Synthesis

Pluronic<sup>®</sup> P123 amphiphilic block copolymer (Aldrich, Saint-Quentin Fallavier, France), urea (Sigma-Aldrich, Saint-Quentin Fallavier, France), zirconium (IV) oxynitrate hydrate (Aldrich, Saint-Quentin Fallavier, France) and copper (II) nitrate hemi(pentahydrate) (Alfa-Aesar Thermo Fisher Lancashire, UK) were dissolved in 375 mL of distilled water. The suspension was heated from room temperature to 95 °C within 30 min under vigorous stirring. After stirring at 95 °C for 48 h, the obtained colloidal solution was aged at 100 °C for 24 h. Then, the material was filtrated, washed with deionized water, and dried at room temperature. Finally, the solid material was calcined at 600 °C for 5 h with a heating rate of 1 °C/min. The obtained material was denoted as Cu-Zr. The iron-containing catalyst was prepared using the same method with the iron nitrate nonahydrate. The dosage of different chemical reagents for synthesis of each catalyst is listed in Table 3 and corresponds to 3 wt% loading of Fe or Cu.

**Table 3.** The chemical dosage used during for the synthesis of Cu-Zr and Fe-Zr catalysts.

Sample	P123/g	Urea/g	ZrO(NO) <sub>3</sub> ·2H <sub>2</sub> O/g	Cu(NO) <sub>2</sub> ·2.5H <sub>2</sub> O/g	Fe(NO) <sub>3</sub> ·9H <sub>2</sub> O/g
Cu-Zr	7.84	7.50	5.03	0.14	-
Fe-Zr	7.84	7.50	5.03	-	0.24

### 3.2. Characterization Techniques

The structural properties of samples were obtained using the X-ray diffraction (XRD) method on a DX-1000 CSC diffractometer (Malvern PANalytical, Shanghai, China), equipped with the Cu K $\alpha$  radiation at 40 kV and 25 mA. The data was recorded in the range  $5^\circ < 2\theta < 90^\circ$  with 0.3 s/step scan speed and  $0.03^\circ$  step size.

Textural properties of the samples were determined by N<sub>2</sub> physisorption at  $-196^\circ\text{C}$  using a Micromeritics (Aachen, Germany) ASAP 2020 instrument. The samples were previously treated in vacuum for 2 h at  $200^\circ\text{C}$ . The data on the specific surface area, mesoporous pore volume and average pore diameter were calculated by the equations of Brunauer–Emmett–Teller (BET), Barrett–Joyner–Halenda (BJH) desorption average pore width (4V/A), and desorption of volume of pores Barrett–Joyner–Halenda (BJH), respectively.

The acidity of samples was examined by NH<sub>3</sub>-TPD using an AUTOCHEM 2910 (Micromeritics, Aachen, Germany). The solid was pre-treated at  $550^\circ\text{C}$  (ramp  $10^\circ\text{C}/\text{min}$ ) during 2 h, under air flow (30 mL/min). Then, it was exposed to 5 vol% NH<sub>3</sub> in He (30 mL/min) for 30 min, and subsequently with He (30 mL/min) for 30 min to remove the physisorbed ammonia. Finally, the NH<sub>3</sub> desorption was performed in helium flow (30 mL/min) from 100 to  $550^\circ\text{C}$  (the heating rate was  $5^\circ\text{C}/\text{min}$ ).

The elemental analysis of sample surface was investigated by X-ray photoelectron spectroscopy (XPS) on a KRATOS spectrometer with an AXIS Ultra DLD (Manchester, UK). All the data were calibrated using the C 1s peak at 284.6 eV, as described elsewhere [43].

### 3.3. Catalytic Tests

The selective catalytic reduction of NO with NH<sub>3</sub> (NH<sub>3</sub>-SCR) was studied in a U-shape glass reactor operating at atmospheric pressure. Prior to the catalytic tests, a catalyst (75 mg) was activated in situ at  $550^\circ\text{C}$  for 30 min in a flow of O<sub>2</sub>/He and then cooled to  $180^\circ\text{C}$ . The following compositions of the gas mixture for NH<sub>3</sub>-SCR of NO: [NO] = 1000 ppm, [NH<sub>3</sub>] = 1000 ppm, [H<sub>2</sub>O] = 3.5 vol%, [O<sub>2</sub>] = 2.5 vol% diluted in helium; total flowrate of 100 mL/min. The tolerance of SO<sub>2</sub> was examined at  $450^\circ\text{C}$  with [SO<sub>2</sub>] = 100 ppm. The weight hourly space velocity (WHSV) was about 80,000 mL/g·h. The SCR was carried out on programmed temperature from 180 to  $550^\circ\text{C}$  with the heating rate  $5^\circ\text{C}/\text{min}$ . The reactants and products were analyzed by a quadruple mass spectrometer (Pfeiffer Omnistar, Saclay, France) equipped with Channeltron and Faraday detectors recording the following masses: NH<sub>3</sub> (m/z = 15, 17, 18), NO (m/z = 30), O<sub>2</sub> (m/z = 16, 32), H<sub>2</sub>O (m/z = 17, 18), N<sub>2</sub> (m/z = 14, 28), N<sub>2</sub>O (m/z = 28, 30, 44), and He (m/z = 4).

The selective catalytic oxidation of NH<sub>3</sub> (NH<sub>3</sub>-SCO) was studied in the U-shape glass reactor operating in similar conditions as described above, using the following gas mixture for NH<sub>3</sub>-SCO: [NH<sub>3</sub>] = 1000 ppm, [H<sub>2</sub>O] = 3.5 vol%, [O<sub>2</sub>] = 2.5 vol% diluted in helium; total flowrate of 100 mL/min. Similarly, the reactants and products were analyzed by a quadruple mass spectrometer (Pfeiffer Omnistar, Saclay, France) equipped with Channeltron and Faraday detectors recording the following masses: NH<sub>3</sub> (m/z = 15, 17, 18), NO (m/z = 30), O<sub>2</sub> (m/z = 16, 32), H<sub>2</sub>O (m/z = 17, 18), N<sub>2</sub> (m/z = 14, 28), N<sub>2</sub>O (m/z = 28, 30, 44), and He (m/z = 4).

## 4. Conclusions

A novel synthesis was proposed for the preparation of zirconia-supported Cu and Fe catalysts. The synthesized catalysts showed promising results in NH<sub>3</sub>-SCR of NO in both the presence and absence of water vapor. The studied materials presented NO reduction with NH<sub>3</sub> which mainly led to N<sub>2</sub> but side reactions resulting in N<sub>2</sub>O and NO<sub>2</sub> formation

were also present. Under hydrothermal conditions NO conversion was lower (<50%) and inferior N<sub>2</sub>O production (ca. 10 ppm) was measured for Cu-Zr and Fe-Zr catalysts, compared to the dry reaction. Furthermore, the Fe-Zr catalyst was highly inactive in NH<sub>3</sub> oxidation during NH<sub>3</sub>-SCR of NO. Regardless of the presence or absence of H<sub>2</sub>O, the Cu and Fe promoted catalysts showed the enhanced resistance in the presence of SO<sub>2</sub>. Feeding SO<sub>2</sub> resulted in an enhanced catalytic performance, suggesting that sulfur dioxide may positively affect the acidity of the ZrO<sub>2</sub>-supported samples. A thorough study is underway to optimize the sulphation of Cu-Zr and Fe-Zr catalysts, coupling FTIR-in situ studies in the presence and absence of SO<sub>2</sub>, for a better understanding of surface, acid-base properties and catalytic behavior.

**Supplementary Materials:** The following are available online at <https://www.mdpi.com/2073-4344/11/1/55/s1>, Figure S1: N<sub>2</sub> selectivity as a function of temperature measured during NH<sub>3</sub>-SCO over Cu-Zr catalyst (A) in absence of water, (B) in presence of water, Fe-Zr catalyst (C) in absence of water, (D) in presence of water, and ZrO<sub>2</sub> support (E) in absence of water, (F) in presence of water. The experimental conditions: [NH<sub>3</sub>] = 1000 ppm, [H<sub>2</sub>O] = 3.5 vol% when used, [O<sub>2</sub>] = 2.5 vol% diluted in helium; total flowrate of 100 ml/min.

**Author Contributions:** Conceptualization, K.Š., P.D.C., and G.D.; methodology, K.Š., Y.W., C.H., L.L., P.D.C., G.D.; validation, K.Š., and G.D.; formal analysis, K.Š., Y.W., C.H., L.L., P.D.C., G.D.; investigation, K.Š., Y.W., L.L., G.D.; resources, C.H., P.D.C., G.D.; writing—original draft preparation, K.Š., Y.W., C.H., P.D.C., G.D.; writing—review and editing, K.Š., Y.W., C.H., L.L., P.D.C., G.D.; supervision, K.Š., C.H., P.D.C., G.D.; project administration, C.H., P.D.C., G.D.; funding acquisition, C.H., G.D. All authors have read and agreed to the published version of the manuscript.

**Funding:** This research received no external funding.

**Institutional Review Board Statement:** Not applicable.

**Informed Consent Statement:** Not applicable.

**Acknowledgments:** We would like to thank Sichuan University and Institut Charles Gerhardt Montpellier, Université de Montpellier, for experimental and characterization facilities.

**Conflicts of Interest:** The authors declare no conflict of interest.

## References

1. Vascellari, M. NO<sub>x</sub> Emission and Mitigation Technologies. In *Handbook of Clean Energy Systems*; John Wiley & Sons: Hoboken, NJ, USA, 2015; pp. 1–23, ISBN 9781118991978.
2. Iwamoto, M.; Furukawa, H.; Mine, Y.; Uemura, F.; Mikuriya, S.I.; Kagawa, S. Copper(II) Ion-exchanged ZSM-5 zeolites as highly active catalysts for direct and continuous decomposition of nitrogen monoxide. *J. Chem. Soc. Ser. Chem. Commun.* **1986**, 1272–1273. [[CrossRef](#)]
3. Ishihara, T.; Ando, M.; Sada, K.; Takiishi, K.; Yamada, K.; Nishiguchi, H.; Takita, Y. Direct decomposition of NO into N<sub>2</sub> and O<sub>2</sub> over La(Ba)Mn(In)O<sub>3</sub> perovskite oxide. *J. Catal.* **2003**, *220*, 104–114. [[CrossRef](#)]
4. Liu, G.; Gao, P.X. A review of NO<sub>x</sub> storage/reduction catalysts: Mechanism, materials and degradation studies. *Catal. Sci. Technol.* **2011**, *1*, 552–568. [[CrossRef](#)]
5. Seo, C.K.; Kim, H.; Choi, B.; Lim, M.T. The optimal volume of a combined system of LNT and SCR catalysts. *J. Ind. Eng. Chem.* **2011**, *17*, 382–385. [[CrossRef](#)]
6. Mrad, R.; Aissat, A.; Cousin, R.; Courcot, D.; Siffert, S. Catalysts for NO<sub>x</sub> selective catalytic reduction by hydrocarbons (HC-SCR). *Appl. Catal. A Gen.* **2015**, *504*, 542–548. [[CrossRef](#)]
7. Breen, J.P.; Burch, R. A review of the effect of the addition of hydrogen in the selective catalytic reduction of NO<sub>x</sub> with hydrocarbons on silver catalysts. *Top. Catal.* **2006**, *39*, 53–58. [[CrossRef](#)]
8. Chen, G.; Xu, J.; Yu, H.; Guo, F.; Xie, J.; Wang, Y. Effect of the non-thermal plasma treatment on the structure and SCR activity of vanadium-based catalysts. *Chem. Eng. J.* **2020**, *380*, 122286. [[CrossRef](#)]
9. Kowalczyk, A.; Świąć, A.; Gil, B.; Rutkowska, M.; Piwowarska, Z.; Borcuch, A.; Michalik, M.; Chmielarz, L. Effective catalysts for the low-temperature NH<sub>3</sub>-SCR process based on MCM-41 modified with copper by template ion-exchange (TIE) method. *Appl. Catal. B Environ.* **2018**, *237*, 927–937. [[CrossRef](#)]
10. Abid, R.; Delahay, G.; Tounsi, H. Selective catalytic reduction of NO by NH<sub>3</sub> on cerium modified faujasite zeolite prepared from aluminum scraps and industrial metasilicate. *J. Rare Earths* **2020**, *38*, 250–256. [[CrossRef](#)]
11. Kieffer, C.; Lavy, J.; Jeudy, E.; Bats, N.; Delahay, G. Characterisation of a commercial automotive NH<sub>3</sub>-SCR copper-zeolite catalyst. *Top. Catal.* **2013**, *56*, 40–44. [[CrossRef](#)]

12. Arfaoui, J.; Ghorbel, A.; Petitto, C.; Delahay, G. A new  $V_2O_5$ - $MoO_3$ - $TiO_2$ - $SO_4^{2-}$  nanostructured aerogel catalyst for diesel DeNOx technology. *New J. Chem.* **2020**, *44*, 16119–16134. [[CrossRef](#)]
13. Leistner, K.; Mihai, O.; Wijayanti, K.; Kumar, A.; Kamasamudram, K.; Currier, N.W.; Yezerets, A.; Olsson, L. Comparison of Cu/BEA, Cu/SSZ-13 and Cu/SAPO-34 for ammonia-SCR reactions. *Catal. Today* **2015**, *258*, 49–55. [[CrossRef](#)]
14. Jabłońska, M.; Delahay, G.; Kruczała, K.; Blachowski, A.; Tarach, K.A.; Brylewska, K.; Petitto, C.; Góra-Marek, K. Standard and fast selective catalytic reduction of NO with  $NH_3$  on zeolites Fe-BEA. *J. Phys. Chem. C* **2016**, *120*, 16831–16842. [[CrossRef](#)]
15. Zhang, L.; Wang, D.; Liu, Y.; Kamasamudram, K.; Li, J.; Epling, W.  $SO_2$  poisoning impact on the  $NH_3$ -SCR reaction over a commercial Cu-SAPO-34 SCR catalyst. *Appl. Catal. B Environ.* **2014**, *156–157*, 371–377. [[CrossRef](#)]
16. Li, Y.; Cheng, H.; Li, D.; Qin, Y.; Xie, Y.; Wang, S.  $WO_3/CeO_2-ZrO_2$  a promising catalyst for selective catalytic reduction (SCR) of NOx with  $NH_3$  in diesel exhaust. *Chem. Commun.* **2008**, 1470–1472. [[CrossRef](#)]
17. Djerad, S.; Geiger, B.; Schott, F.J.P.; Kureti, S. Synthesis of nano-sized  $ZrO_2$  and its use as catalyst support in SCR. *Catal. Commun.* **2009**, *10*, 1103–1106. [[CrossRef](#)]
18. Apostolescu, N.; Geiger, B.; Hizbullah, K.; Jan, M.T.; Kureti, S.; Reichert, D.; Schott, F.; Weisweiler, W. Selective catalytic reduction of nitrogen oxides by ammonia on iron oxide catalysts. *Appl. Catal. B Environ.* **2006**, *62*, 104–114. [[CrossRef](#)]
19. Shen, B.; Zhang, X.; Ma, H.; Yao, Y.; Liu, T. A comparative study of Mn/ $CeO_2$ , Mn/ $ZrO_2$  and Mn/Ce- $ZrO_2$  for low temperature selective catalytic reduction of NO with  $NH_3$  in the presence of  $SO_2$  and  $H_2O$ . *J. Environ. Sci.* **2013**, *25*, 791–800. [[CrossRef](#)]
20. Peng, B.; Rappé, K.G.; Cui, Y.; Gao, F.; Szanyi, J.; Olszta, M.J.; Walter, E.D.; Wang, Y.; Holladay, J.D.; Goffe, R.A. Enhancement of high-temperature selectivity on Cu-SSZ-13 towards  $NH_3$ -SCR reaction from highly dispersed  $ZrO_2$ . *Appl. Catal. B Environ.* **2020**, *263*. [[CrossRef](#)]
21. Verdier, S.; Rohart, E.; Bradshaw, H.; Harris, D.; Bichon, P.; Delahay, G. Acidic zirconia materials for durable  $NH_3$ -SCR deNOx catalysts. *SAE Tech. Pap.* **2008**, *1*, 1022.
22. Delahay, G.; Ensuque, E.; Coq, B.; Figuéras, F. Selective catalytic reduction of nitric oxide by n-decane on Cu/sulfated-zirconia catalysts in oxygen rich atmosphere: Effect of sulfur and copper contents. *J. Catal.* **1998**, *175*, 7–15. [[CrossRef](#)]
23. Delahay, G.; Coq, B.; Ensuque, E.; Figuéras, F. Catalytic behaviour of Cu/ $ZrO_2$  and Cu/ $ZrO_2(SO_4^{2-})$  in the reduction of nitric oxide by decane in oxygen-rich atmosphere. *Catal. Lett.* **1996**, *39*, 105–109. [[CrossRef](#)]
24. Figueras, F.; Coq, B.; Ensuque, E.; Tachon, D.; Delahay, G. Catalytic properties of Cu on sulphated zirconias for DeNOx in excess of oxygen using n-decane as reductant. *Catal. Today* **1998**, *42*, 117–125. [[CrossRef](#)]
25. Pasel, J.; Speer, V.; Albrecht, C.; Richter, F.; Papp, H. Metal doped sulfated  $ZrO_2$  as catalyst for the selective catalytic reduction (SCR) of NO with propane. *Appl. Catal. B Environ.* **2000**, *25*, 105–113. [[CrossRef](#)]
26. Pietrogiamomi, D.; Sannino, D.; Magliano, A.; Ciambelli, P.; Tuti, S.; Indovina, V. The catalytic activity of  $CuSO_4/ZrO_2$  for the selective catalytic reduction of NOx with  $NH_3$  in the presence of excess  $O_2$ . *Appl. Catal. B Environ.* **2002**, *36*, 217–230. [[CrossRef](#)]
27. Pietrogiamomi, D.; Magliano, A.; Sannino, D.; Campa, M.C.; Ciambelli, P.; Indovina, V. In situ sulphated  $CuO_x/ZrO_2$  and  $CuO_x/sulphated-ZrO_2$  as catalysts for the reduction of NOx with  $NH_3$  in the presence of excess  $O_2$ . *Appl. Catal. B Environ.* **2005**, *60*, 83–92. [[CrossRef](#)]
28. Ismail, R.; Arfaoui, J.; Ksibi, Z.; Ghorbel, A.; Delahay, G. Effect of the iron amount on the physicochemical properties of Fe- $ZrO_2$  aerogel catalysts for the total oxidation of toluene in the presence of water vapor. *J. Porous Mater.* **2020**, *27*, 1847–1852. [[CrossRef](#)]
29. Navío, J.A.; Hidalgo, M.C.; Colón, G.; Botta, S.G.; Litter, M.I. Preparation and physicochemical properties of  $ZrO_2$  and Fe/ $ZrO_2$  prepared by a sol-gel technique. *Langmuir* **2001**, *17*, 202–210. [[CrossRef](#)]
30. López-Hernández, I.; Mengual, J.; Palomares, A.E. The influence of the support on the activity of Mn-Fe catalysts used for the selective catalytic reduction of NOx with ammonia. *Catalysts* **2020**, *10*, 63. [[CrossRef](#)]
31. Kustov, A.L.; Rasmussen, S.B.; Fehrmann, R.; Simonsen, P. Activity and deactivation of sulphated  $TiO_2$ - and  $ZrO_2$ -based V, Cu, and Fe oxide catalysts for NO abatement in alkali containing flue gases. *Appl. Catal. B Environ.* **2007**, *76*, 9–14. [[CrossRef](#)]
32. Indovina, V.; Campa, M.C.; Pepe, F.; Pietrogiamomi, D.; Tuti, S. Iron species in  $FeO_x/ZrO_2$  and  $FeO_x/sulphated-ZrO_2$  catalysts. *Stud. Surf. Sci. Catal.* **2005**, *155*, 329–337. [[CrossRef](#)]
33. Fan, B.; Zhang, Z.; Liu, C.; Liu, Q. Investigation of sulfated iron-based catalysts with different sulfate position for selective catalytic reduction of NOx with  $NH_3$ . *Catalysts* **2020**, *10*, 1035. [[CrossRef](#)]
34. Liu, C.; Wang, H.; Bi, Y.; Zhang, Z. A study on the selective catalytic reduction of NOx: by ammonia on sulphated iron-based catalysts. *RSC Adv.* **2020**, *10*, 40948–40959. [[CrossRef](#)]
35. Yu, Z.; Liu, B.; Zhou, H.; Feng, C.; Wang, X.; Yuan, K.; Gan, X.; Zhu, L.; Zhang, G.; Xu, D. Mesoporous  $ZrO_2$  fibers with enhanced surface area and the application as recyclable absorbent. *Appl. Surf. Sci.* **2017**, *399*, 288–297. [[CrossRef](#)]
36. Gao, S.; Chen, X.; Wang, H.; Mo, J.; Wu, Z.; Liu, Y.; Weng, X. Ceria supported on sulfated zirconia as a superacid catalyst for selective catalytic reduction of NO with  $NH_3$ . *J. Colloid Interface Sci.* **2013**, *394*, 515–521. [[CrossRef](#)] [[PubMed](#)]
37. Kogler, M.; Köck, E.M.; Vanicek, S.; Schmidmair, D.; Götsch, T.; Stöger-Pollach, M.; Hejny, C.; Klötzer, B.; Penner, S. Enhanced kinetic stability of pure and Y-doped tetragonal  $ZrO_2$ . *Inorg. Chem.* **2014**, *53*, 13247–13257. [[CrossRef](#)]
38. Tan, D.; Lin, G.; Liu, Y.; Teng, Y.; Zhuang, Y.; Zhu, B.; Zhao, Q.; Qiu, J. Synthesis of nanocrystalline cubic zirconia using femtosecond laser ablation. *J. Nanoparticle Res.* **2011**, *13*, 1183–1190. [[CrossRef](#)]
39. Boroń, P.; Chmielarz, L.; Dzwigaj, S. Influence of Cu on the catalytic activity of FeBEA zeolites in SCR of NO with  $NH_3$ . *Appl. Catal. B Environ.* **2015**, *168–169*, 377–384. [[CrossRef](#)]

40. Du, L.; Wang, W.; Yan, H.; Wang, X.; Jin, Z.; Song, Q.; Si, R.; Jia, C. Copper-ceria sheets catalysts: Effect of copper species on catalytic activity in CO oxidation reaction. *J. Rare Earths* **2017**, *35*, 1186–1196. [[CrossRef](#)]
41. Shannon, R.D. Revised effective ionic radii and systematic studies of interatomic distances in halides and chalcogenides. *Acta Crystallogr. Sect. A Cryst. Phys. Diffr. Theor. Gen. Crystallogr.* **1976**, *32*, 751–767. [[CrossRef](#)]
42. Breviglieri, S.T.; Cavalheiro, É.T.G.; Chierice, G.O. Correlation between ionic radius and thermal decomposition of Fe(II), Co(II), Ni(II), Cu(II) and Zn(II) diethanoldithiocarbamates. *Thermochim. Acta* **2000**, *356*, 79–84. [[CrossRef](#)]
43. Wang, Y.; Zhao, Q.; Wang, Y.; Hu, C.; Da Costa, P. One-Step synthesis of highly active and stable Ni-ZrOx for dry reforming of methane. *Ind. Eng. Chem. Res.* **2020**, *59*, 11441–11452. [[CrossRef](#)]
44. Khorsand Zak, A.; Abd Majid, W.H.; Abrishami, M.E.; Yousefi, R. X-ray analysis of ZnO nanoparticles by Williamson-Hall and size-strain plot methods. *Solid State Sci.* **2011**, *13*, 251–256. [[CrossRef](#)]
45. Williamson, G.K.; Hall, W.H. X-ray line broadening from fcc aluminium and wolfram. *Acta Metall.* **1953**, *1*, 22–31. [[CrossRef](#)]
46. Ismail, R.; Arfaoui, J.; Ksibi, Z.; Ghorbel, A.; Delahay, G. Ag/ZrO<sub>2</sub> and Ag/Fe-ZrO<sub>2</sub> catalysts for the low temperature total oxidation of toluene in the presence of water vapor. *Transit. Met. Chem.* **2020**, *45*, 501–509. [[CrossRef](#)]
47. Lee, S.M.; Park, K.H.; Hong, S.C. MnOx/CeO<sub>2</sub>-TiO<sub>2</sub> mixed oxide catalysts for the selective catalytic reduction of NO with NH<sub>3</sub> at low temperature. *Chem. Eng. J.* **2012**, *195–196*, 323–331. [[CrossRef](#)]
48. Zhao, H.; Wang, Y.; Wang, Y.; Cao, T.; Zhao, G. Electro-Fenton oxidation of pesticides with a novel Fe<sub>3</sub>O<sub>4</sub>@Fe<sub>2</sub>O<sub>3</sub>/activated carbon aerogel cathode: High activity, wide pH range and catalytic mechanism. *Appl. Catal. B Environ.* **2012**, *125*, 120–127. [[CrossRef](#)]
49. Wang, Y.; Li, L.; Wang, Y.; Da Costa, P.; Hu, C. Highly carbon-resistant Y doped NiO-ZrO<sub>m</sub> catalysts for dry reforming of methane. *Catalysts* **2019**, *9*, 1055. [[CrossRef](#)]
50. Sutthiumporn, K.; Maneerung, T.; Kathiraser, Y.; Kawi, S. CO<sub>2</sub> dry-reforming of methane over La<sub>0.8</sub>Sr<sub>0.2</sub>Ni<sub>0.8</sub>M<sub>0.2</sub>O<sub>3</sub> perovskite (M = Bi, Co, Cr, Cu, Fe): Roles of lattice oxygen on C-H activation and carbon suppression. *Int. J. Hydrogen Energy* **2012**, *37*, 11195–11207. [[CrossRef](#)]
51. Jiang, H.; Zhou, J.; Wang, C.; Li, Y.; Chen, Y.; Zhang, M. Effect of cosolvent and temperature on the structures and properties of Cu-MOF-74 in low-temperature NH<sub>3</sub>-SCR. *Ind. Eng. Chem. Res.* **2017**, *56*, 3542–3550. [[CrossRef](#)]
52. Khodayari, R.; Odenbrand, C.U.I. Regeneration of commercial SCR catalysts by washing and sulphation: Effect of sulphate groups on the activity. *Appl. Catal. B Environ.* **2001**, *33*, 277–291. [[CrossRef](#)]
53. Miao, J.; Li, H.; Su, Q.; Yu, Y.; Chen, Y.; Chen, J.; Wang, J. The combined promotive effect of SO<sub>2</sub> and HCl on Pb-poisoned commercial NH<sub>3</sub>-SCR V<sub>2</sub>O<sub>5</sub>-WO<sub>3</sub>/TiO<sub>2</sub> catalysts. *Catal. Commun.* **2019**, *125*, 118–122. [[CrossRef](#)]
54. Yu, Y.; Wang, J.; Chen, J.; Meng, X.; Chen, Y.; He, C. Promotive Effect of SO<sub>2</sub> on the activity of a deactivated commercial selective catalytic reduction catalyst: An in situ DRIFT study. *Ind. Eng. Chem. Res.* **2014**, *53*, 16229–16234. [[CrossRef](#)]